An Analysis of 20 Years of Meteorological and Oceanographic Data from Ocean Station N

CLIVE E. DORMAN,[1] C. A. PAULSON AND W. H. QUINN

School of Oceanography, Oregon State University, Corvallis 97331

(Manuscript received 18 March 1974, in revised form 28 June 1974)

ABSTRACT

Meteorological and oceanographic data for Ocean Station Vessel *N* (30N, 140W) are analyzed over 20 years (1951–70) and 7 years (1964–70), respectively. A rainfall estimate is constructed for the 20-year period. The yearly average rainfall is 23 cm, far less than existing estimates. Daily and seasonal variations are presented. Heat budgets of the surface show that the two decades (1951–60, 1961–70) are distinctly different. Anomalies of the 20 years of all meteorological variables are calculated. The pressure anomaly appears to be loosely correlated with anomalous large-scale events in the equatorial Pacific. Time series cross sections are shown of the mixed layer depth, bottle temperature and salinity. The near-surface density appears to be largely controlled by temperature.

1. Introduction

The best available data for investigating the long-term characteristics of the relation between atmospheric and oceanic structure far removed from land are observations made by ocean weather ships. It is the purpose of this paper to describe the results of analyses of 20 years of oceanographic and meteorological observations from Ocean Station *N* (hereafter referred to as *N*) located at 30N, 140W in the eastern subtropical Pacific. The time series are related to climatic events. Seasonal and diurnal variations are analyzed, the heat budget is computed, and the evolution of the structure of the oceanic mixed layer is described.

2. Observations

The climate and weather at *N* can best be described as moderate. Although there are seasonal variations, the average annual temperature range is about 6C and the maximum wind speed for a month infrequently exceeds 30 kt. The lower atmosphere is typically capped by an inversion with a base between 900 and 850 mb. Stratiform clouds below the inversion, which constitute most of the total cloud cover, can yield light rain or drizzle. There is a high degree of cloudiness all year. Thunderstorms are infrequent and the total yearly precipitation is about 23 cm.

The North Pacific subtropical high maintains the inversion at Ocean Station *N* except during frontal passages. Frontal passages occur most frequently during the winter. Storm centers associated with the fronts usually pass to the north but occasionally pass close to *N*, particularly in winter. Tropical storms are rare. Disturbances are infrequent during the summer.

Ocean Station *N* lies in the center of the east North Pacific Central Water mass (Sverdrup *et al.*, 1942). The depth of the mixed layer is about 20 m during the summer, increasing to 140 m in the late winter. Below the mixed layer, temperature decreases rapidly with depth for at least 20–50 m. At depths >250 m the temperature decreases slowly. Salinity is a maximum at the surface and decreases with depth to 500 m, then slowly increases with depth. There might also be a small local minimum of salinity at 200 m except during the summer (Husby, 1969).

The Station usually lies on the perimeter of current gyres. According to the *Climatological and Oceanographic Atlas for Mariners* (U. S. Naval Hydrographic Office, 1961), there is a seasonal variation in surface currents. During winter, *N* is at the eastern extremity of a large anticyclonic current gyre with a current at *N* to the south or southwest of 0.1–0.3 kt. During summer, *N* is at the southern edge of a smaller anticyclonic gyre centered at about 40N, 140W, with currents at *N* to the southwest at 0.1–0.3 kt. The current pattern during transition between summer and winter is not certain. Drogue measurements in September, reported by Husby (1969), indicated a westward current of 0.3 kt. Large wire angles have been noted during hydrographic casts at *N*, suggesting occasional strong currents.

The meteorological data analyzed in this study were observed at *N* from 1951 to 1970. The average position of *N* in 1951 was 33N, 135W. In 1952 and 1953 *N* was at 32.5N, 135W. For the first 10 weeks of 1954 the average position of *N* was 31N, 140W. During the

[1] Present affiliation: Department of Geology, San Diego State University.

remainder of the period 1954 to 1970, the average position was at 30N, 140W.

Meteorological observations were taken every 3 hr beginning at 0000 GMT each day. They included wind speed, wind direction, pressure, water temperature, dew point, air temperature, lower cloud cover, total cloud cover, and present weather. Water temperature was not observed during 1952 and the first half of 1953. Dew point was observed four to six times a day from 1953 to mid 1963. Less than 2% of all remaining observations (all variables) were missing.

A description of the meteorological and oceanographic instrumentation, location of instruments, and methods of observation is given in various U. S. government manuals, some of which are available from the Superintendent of Documents, U. S. Government Printing Office (personal communication, Marine Sciences Branch, U. S. Coast Guard, Pacific Area, San Francisco). Wind speed and direction were measured by a propeller-anemometer/wind vane combination located at a height of about 25 m above mean sea level. Water temperature was measured with a bucket and mercury thermometer. Air temperature and dew point were measured with a sling psychrometer on the bridge at a height of about 10 m above mean sea level.

The oceanographic data (apart from the water temperature observations) considered here are from the 7-year period, 1964–70. All of the observations at *N* during this period of time are used, both bathythermograph (BT) and hydrocast observations (salinity samples and temperature from reversing thermometers). In addition, BT and hydrocast data from other ships were used if taken within 4° of 30N, 140W and between 1964 and 1970. These additional observations amount to only a few percent of the total. The frequency of BT and hydrocast observations was highly variable, especially the hydrocasts which were sporadic during 1964–66, but which were at least as often as one every 3 days during 1970. The number of BT's per year ranged from 675 in 1970 to a high of 1800 in 1964.

3. Seasonal Variability

The seasonal variation of meteorological variables and bucket water temperature are shown in Figs. 1 and 2. Each point is obtained by averaging observations over each day of the year and each particular day over the 20-year period. The resulting time series is smoothed by a 7-day running mean.

Bucket water temperature, air temperature and dew point are highly correlated, showing a minimum in March and a maximum in September (Fig. 1). The sea-air temperature difference is positive throughout the year, but larger in winter than in summer.

The rainfall rate estimate in Fig. 2 is constructed from the present weather part of the synoptic observations by use of a method suggested by Tucker (1961). The rainfall rate is a maximum in winter and has a broad minimum in summer. An unexpected result is that the yearly total is 23 cm, less that one-half and one-fifth that suggested for the vicinity of *N* by Jacobs (1951) and Budyko (1956), respectively. Reed and Elliott (1973) have expanded the use of Tucker's technique for rainfall estimates to other stations in the Pacific and constructed estimates which are also much lower than previous estimates.

The seasonal variation of wind speed is similar to that for rainfall with a maximum in winter and a minimum in summer. Some of the small-scale fluctuations of wind speed and rainfall are also positively correlated, indicating, as one might expect, that anomalously high winds are associated with high rainfall. The average wind speed at any time of the year varies between 9 and 17 kt.

Cloud cover shows little seasonal variation except for a decrease of about 1/8 in August, then a gradual increase to a nearly constant value from January through July of about 6/8. On the average more than 4/8 of the observed total cloud cover is low cloud.

Pressure exhibits a double minimum, one in late January and another in October. It has a broad maximum from March to July. The minimum in January–February coincides with maximum wind speeds. The mechanisms causing the secondary maximum of pressure in December and early January are obscure.

Seasonal variation of the oceanic surface variables is shown in the lower four curves of Fig. 2 for the period 1964–70. The depth of the mixed layer, denoted by

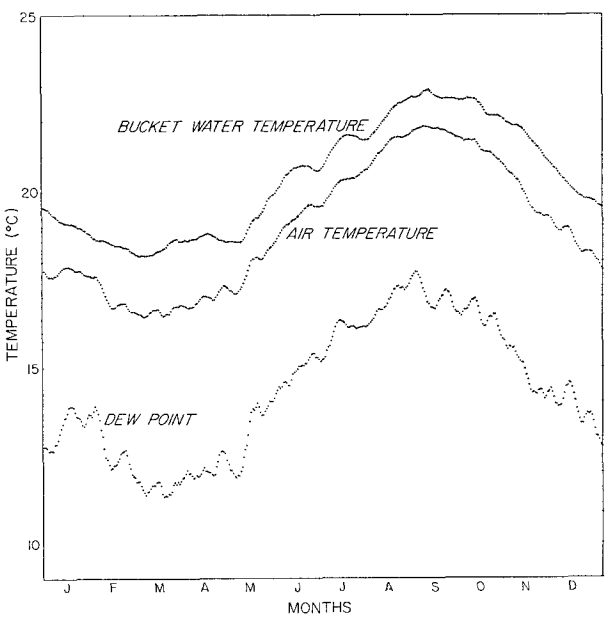

FIG. 1. Seasonal variations of bucket water temperature, air temperature, and dew point temperature. Each point is a daily average of observations from 1951–70 smoothed by a 7-day running average.

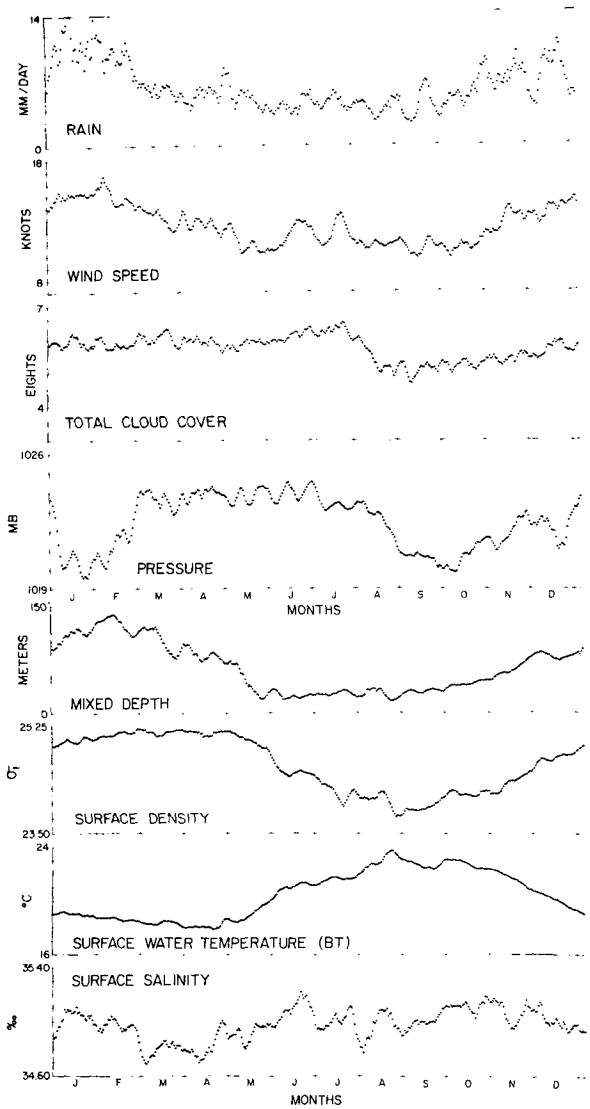

FIG. 2. Seasonal variation of rainfall rate, wind speed, total cloud cover, pressure, mixed depth (oceanic), surface density, water temperature (BT), and surface salinity. Each point is a daily average of observations smoothed by a 7-day running average (meteorological data 1951–70; oceanographic data 1964–70).

"mixed depth," is defined as the depth at which a BT temperature is 0.2C less than the surface temperature from the same BT. The maximum mixed depth occurs in February and the summer minimum is at 20 m. These contrast with Bathen (1972) who shows the area around N to have a May maximum mixed layer depth of 140 m and a summer minimum of 50 m. Surface water temperature variation is similar to the bucket water temperature as ought to be the case. Dissimilarities are likely due to the different number of years averaged. Surface density (σ_t) is a near mirror image of surface temperature, indicating that salinity is of minor importance in determining density. Salinity shows very little seasonal variation. But, individual years do show minima in February and March and maxima in late summer.

A time-depth cross section showing mean seasonal temperature structure is given in Fig. 3. The temperatures are from BT's averaged over the period 1964–70 and smoothed by a 2-week running mean. The outstanding feature is the development of a warm, shallow, nearly isothermal layer in the early summer which increases in temperature during the summer and then cools and deepens in the fall and winter, reaching a depth of about 125 m in late winter. The small-scale structure is statistically insignificant. Seasonal temperature structure at N is similar to that further north at Ocean Surface Vessel Papa (Tully and Giovando, 1963) but the amplitude of the seasonal temperature variation is less, 5C compared to 11C further north, and the maximum and minimum surface temperatures at N occur about a month later. Evolution of the mixed layer is similar except for a delay of about a month at N for the beginning of the deepening of the mixed layer. The average maximum depth of the mixed layer which occurs in late winter is about 120 m for both locations.

A time-depth section of salinity is shown in Fig. 4. There is little evidence of any seasonal variation, even at the surface where one might expect variations due to variations in evaporation. The seasonal density structure (not shown) is very similar to temperature. Salinity plays an insignificant role in determining seasonal fluctuations of density at N.

4. Surface heat balance

Empirical formulas are used to estimate the heat fluxes at the sea surface. The incoming solar shortwave radiation is estimated by Berlyand (1960) as

$$Q_{\text{short}}=rs(1-aC-a^2C^2), \qquad (1)$$

where r is the reflection coefficient, s the clear sky radiation at the surface, C the fraction of total cloud

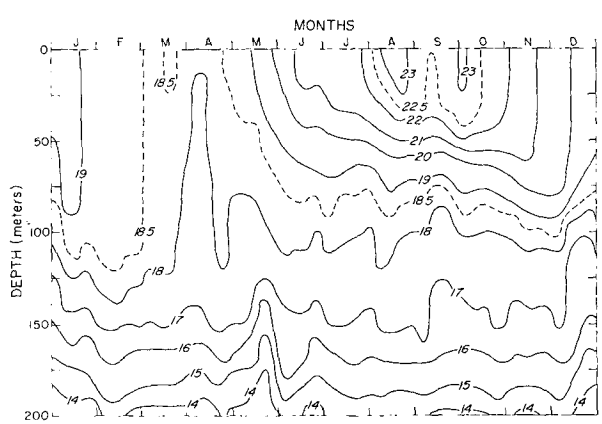

FIG. 3. Seasonal depth cross section of water temperature (°C) from hydrocasts for 1964–70.

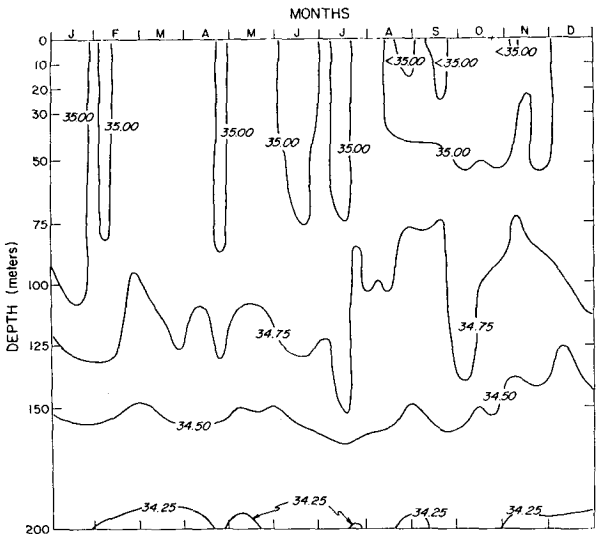

FIG. 4. Seasonal depth cross section of salinity (‰) from hydrocasts for 1964–70.

cover, and a an empirical constant which is the function of latitude. The above formula was also used by Wyrtki (1965) in his study of the heat balance of the North Pacific. But, in our case, the lower cloud amount was used in place of total cloud amount C to approach a heat balance. Higher clouds contributed, on the average, only about 1/8 of the total cloud cover. However, including them in C has a disproportionately large effect on estimated incoming solar radiation since they are often cirrus type and more transparent to solar radiation than the dominant lower cloud. For back radiation, the following formula was used (Wyrtki, 1965):

$$Q_{\text{back}}=\sigma T_w^4(a-be_a^{\frac{1}{2}})(1-cC^2)+dT_w^3(T_w-T_a), \quad (2)$$

where σ is the Stefan-Boltzmann constant, T_w the surface water temperature, e_a the vapor pressure of the air, and a, b, c and d empirical constants (values given by Wyrtki). Sensible and latent heat fluxes were calculated from the standard bulk transfer formulas (e.g., Malkus, 1962):

$$Q_{\text{sen}}=\rho c_p C_H(T_w-T_a)u_a, \quad (3)$$

$$Q_{\text{evap}}=\rho C_E L(q_s-q_a)u_a, \quad (4)$$

where ρ is the air density, c_p the heat capacity at constant pressure, C_H and C_E the bulk exchange coefficients, u_a the wind speed, L the latent heat of evaporation, q_s the saturation specific humidity at the surface temperature, and q_a the specific humidity of the air. C_H and C_E are assumed equal to the drag coefficient for neutral conditions and are assumed to vary with bulk stability according to Deardoroff (1968). A drag coefficient of 1.3×10^{-3} referenced to observations at 10 m height was assumed for the neutral case. The neutral exchange coefficients were corrected assuming a log profile for the wind speed measurements at 25 m. The temperature and dew point were measured at 10 m. Calculations showed that the effect of stability on the exchange coefficients was typically less than 5% as a result of the limited deviations from neutral stability at N. Heat balance at the surface is given by

$$Q_{\text{bal}}=Q_{\text{short}}-Q_{\text{evap}}-Q_{\text{back}}-Q_{\text{sen}}. \quad (5)$$

The above empirical formulas were applied to the 3-hr values of the observed variables at N for the period 1951–70. Average seasonal variations of the fluxes and balance are shown in Fig. 5 for the two decades, 1951–60 and 1961–70. The heat balance is dominated by the gain of solar radiation and the

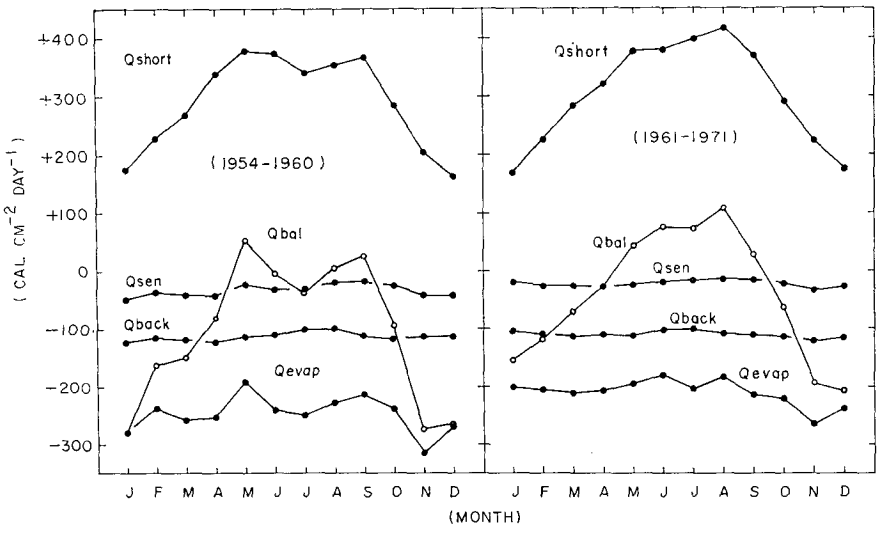

FIG. 5. Heat balance for the two decades, 1951–60, 1961–70: Q_{short} is the downward short-wave radiation, Q_{sen} the upward sensible heat flux, Q_{back} the net upward longwave radiation, Q_{evap} the upward latent heat flux, and Q_{bal} the total heat flux gain by the surface.

loss of the flux of latent heat. The sensible heat flux is small, about one-tenth of the latent heat flux, and is a maximum during winter in the first decade but shows very little variation in the second decade. The variation of latent heat flux is also larger in the first decade, reaching a maximum in the winter.

The average heat balance for the two decades is distinctly different. The first decade has a mean deficit of 90 ly day^{-1} while the second decade has a deficit of 40 ly day^{-1}. The 1951–60 decade may be partly affected by *N* being located 3° north of its regular station from 1951–53. However, the rest of the decade shows the same approximate annual deficit as 1951–53.

5. Anomalies

Twenty-year time series of deviations from the mean, called anomalies, were constructed for various observed meteorological parameters as shown in Fig. 6. These time series (excepting rainfall rate) represent deviations, following smoothing of weekly averages, from 20-year weekly means. The curves (excepting rainfall) have

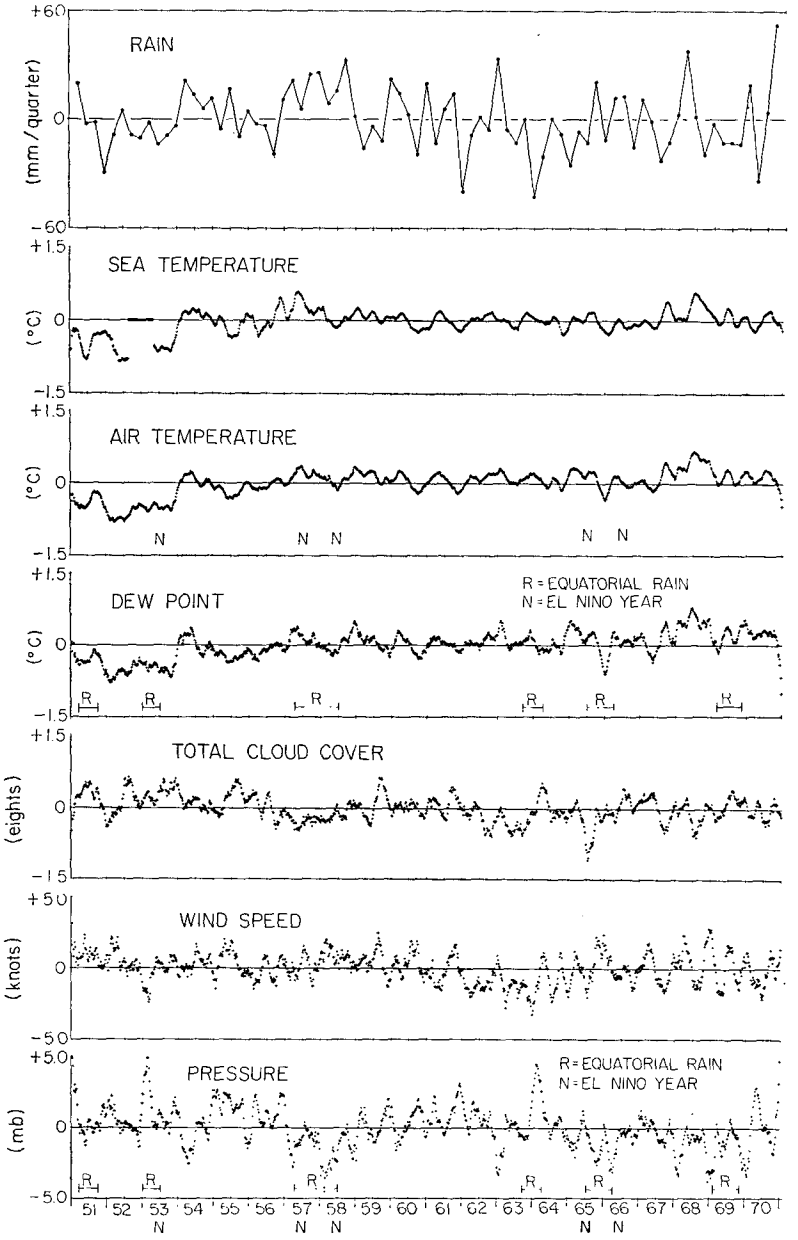

FIG. 6. Time series of weekly means expressed as departures from the mean and smoothed by a 13-week running mean.

been smoothed by a 13-week running mean. The 13-week running mean was selected as it filters out the sub-seasonal fluctuations, most of which appear to be spurious.

Precipitation is estimated using Tucker's (1961) method. The deviation from the quarterly average (rather than weekly) is plotted. Due to the uncertain nature of the rainfall estimate, a quarterly average was selected in order to have each point based upon enough data so as to have some statistical significance.

In discussing the anomalies, the period before 1954 will be ignored as *N* was 3° north of its regular station. Certain climatic events in the equatorial Pacific for the period 1951–70 are shown in the anomaly graph. These events include El Niño and abnormally high rainfall in the equatorial Pacific dry zone (Quinn and Burt, 1972). El Niño is the term for anomalously warm water invasions associated with cessation of upwelling off the coast of Peru.

Anomalies of sea temperature, air temperature and dew point are highly correlated and in phase. The only period in which the sea surface temperature anomaly significantly exceeds that of the air temperature and dew point is during the 1957–58 winter which coincided with a large-scale warming of the North Pacific (Namias, 1959; Bjerknes, 1969), and the most disastrous El Niño of the 1951–70 period (Quinn and Burt, 1972).

The most extreme variations can be seen in the pressure plots. Pressure may possibly be correlated with extreme equatorial developments. The largest and longest negative pressure anomaly is associated with the 1957–58 equatorial rainfall and the most extreme El Niño of the 1951–70 period. A large negative anomaly (more than −2.5 mb) is also associated with the weak El Niño of 1965 and the equatorial rainfall of 1965–66. However, further relationships appear to be meaningless. The unusual 1957–58 rainfall also coincides with the extreme El Niño.

In addition to the meteorological anomalies, surface heat flux anomalies were constructed. Because of the difference in the heat balances, the heat flux anomalies were divided into the two decades 1951–60 and 1961–70 for reasons discussed in the previous section. In Fig. 7, each point is the monthly heat flux computed from the 3-hr meteorological values, further smoothed by a 3-month running mean.

The heat balance is largely a reflection of the solar energy gain balanced by the loss to evaporation. Sensible heat and back radiation fluxes are minor components of the heat balance, although they are in phase with the latent heat flux. Latent heat and shortwave heat fluxes are generally in phase from 1953 to 1958, and 1966 to 1970, while they are generally out of phase from 1959–65.

6. Diurnal variations

The diurnal variation typical of a subtropical station is investigated by averaging together all of the 20 years of observations for a parameter for each of the eight 3-hr observations in a day. Observations for a day were included only if all eight observations for that day were available so as to eliminate any bias for a particular hour. Average deviation from the daily mean of the meteorological variables is shown in Fig. 8. Diurnal range, average and standard deviation of the

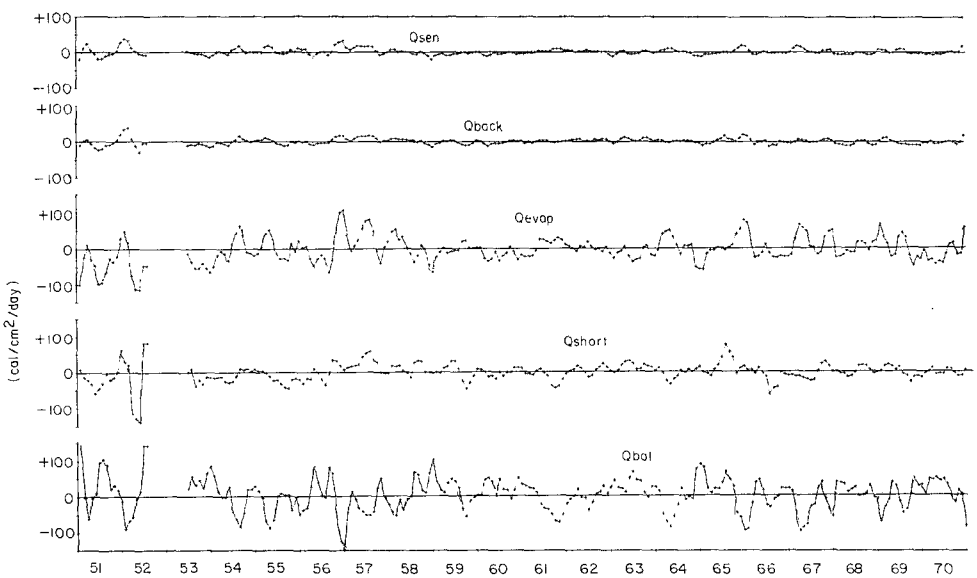

FIG. 7. Time series of monthly means of the heat balance expressed as departures from the mean (1951–60 and 1961–70, respectively) and smoothed by a 5-month running mean. See legend to Fig. 5 for definition of terms.

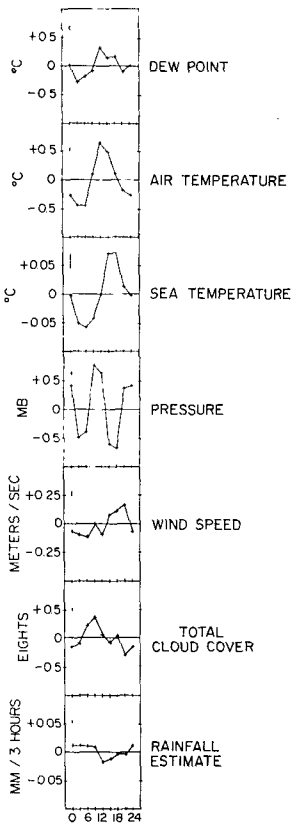

FIG. 8. Diurnal variations expressed as departures from the daily mean. Time is local.

variables for the seasons are given in Table 1 and in the figures. In the upper left hand corner of each figure section is an error bar which is the largest standard deviation on that curve divided by the square root of the number of observations.

The diurnal variation of the sea temperature of each of the seasons has the same shape as the average for all seasons. There is a minimum of the sea temperature at 0600 LT and a maximum between 1500 and 1800 LT. The range for the winter is about half that of the other three seasons. Diurnal variation of the sea temperature for these latitudes is one-half that suggested by Roll (1965).

As with the sea temperature, the shape of the air temperature diurnal variation curve is the same for all seasons. Deviation from the daily mean of the air temperature shows a minimum between 0300 and 0600 LT, and a maximum at 1200. A part of the diurnal variation may be due to radiation errors (c.f. Roll, 1965).

Somewhat similar to the sea and air temperature is the deviation from the daily mean of the dew point. Also, shapes of all seasonal curves are the same so the average for all seasons is shown. Dew point deviation from the daily mean has a minimum at 0300 LT and a maximum at 1200. The plateau in the dew point between 1500 and 1800 appears in each of the seasonal curves.

The deviation from the daily mean of the surface pressure has a symmetrical semidiurnal variation. All curves of the pressure have the same shape. Not shown are the graphs of the spring and summer diurnal variations which have similar means and ranges. The minima are between 0300 and 0600 and 1500 and 1800, while the maxima are between 0900 and 1200 and 2100 and 2400.

Since all four seasons of the deviation from the daily mean of the diurnal wind speed are distinctly different, all are shown in Fig. 9. The wind speed has a minimum at 1200 LT for all seasons and another minimum at 0600 for all seasons except winter. The apparent minima in the winter diurnal variation at 0300 and 1800 are not significant. Fall has an additional minimum at 0000. In the spring, the wind speed shows a maximum at 1800, while in summer and fall it is at 2100. The spring, summer and fall have a local minimum at 1200,

TABLE 1. Statistics for the diurnal deviation from the daily mean.

Variable	Season	Daily mean	Daily range	Daily average standard deviation
Wind	W	7.3	0.15	3.59
(m sec^{-1})	S	6.7	0.36	3.28
	S	5.7	0.46	2.69
	F	5.4	0.35	2.91
	avg.	6.2	0.31	3.22
Pressure*	W	1.6	1.9	6.48
(mb)	S	3.5	1.5	5.67
	S	3.6	1.4	2.77
	F	0.9	1.6	3.52
	avg.	2.4	1.4	5.01
Total cloud	W	5.74	0.70	2.29
cover	S	5.93	0.72	2.27
(eights)	S	6.02	0.87	2.21
	F	5.19	0.71	2.44
	avg.	5.72	0.64	2.33
T_{Sea}	W	19.71	0.08	1.24
(°C)	S	18.52	0.15	0.99
	S	20.92	0.17	1.54
	F	22.43	0.15	1.16
	avg.	20.41	0.13	1.91
T_{Air}	W	18.17	0.90	1.69
(°C)	S	16.86	1.12	1.53
	S	19.76	1.19	1.67
	F	21.29	1.14	1.32
	avg.	19.01	1.08	2.28
T_{Dew}	W	13.76	0.55	3.08
(°C)	S	12.22	0.68	2.68
	S	15.87	0.56	2.28
	F	17.02	0.61	2.29
	avg.	14.76	0.60	3.18
Rain	W	0.11	0.02	0.487
estimate	S	0.08	0.03	0.367
[mm (3 hr)$^{-1}$]	S	0.06	0.05	0.269
	F	0.06	0.04	0.324
	avg.	0.08	0.03	0.374

* Actual value minus 1020 mb.

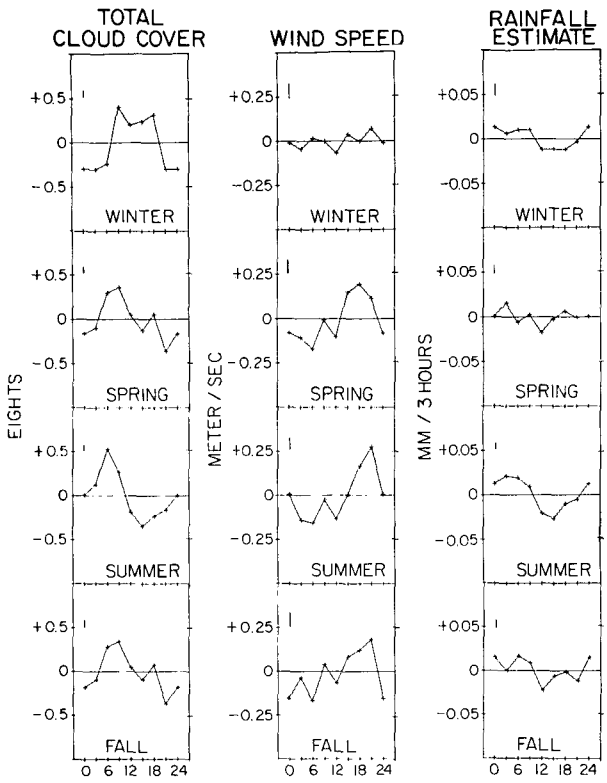

FIG. 9. Diurnal variations of the wind speed, cloud cover and rainfall rate, expressed as departures from the daily mean for four seasons.

while the fall has an additional local maximum at 0300. It is interesting to note that the winter range is at least half that of the other seasons. From these data, a slight semidiurnal trend can be seen in the variation of the wind speed, particularly during spring through fall, which is to be expected (Roll, 1965). But the range of the diurnal variation of wind speed at N is only about half that suggested by Roll (1965) as typical of these latitudes.

Another complicated diurnal variation is that of the total cloud cover (Fig. 9). The winter diurnal variation of the total cloud cover has a maximum at 0900 LT and a local maximum at 1800. Spring and fall are exactly the same with a minimum at 1500 and 2100, as well as maxima at 0900 and 1800. The summer has one maximum at 0600 and one minimum at 1500. It should be recalled that there is a bias by the observer to report lesser cloud amounts at night because nighttime clouds cannot be as easily detected.

The last diurnal variation to be considered here is that of the rainfall rate estimate (Fig. 9). A rain estimate is derived from the "present weather" part of the synoptic observation by the method previously described. The graphs are constructed in the same manner as the previous diurnal trends, except that the vertical axis is ± 0.01 mm $(3\ \text{hr})^{-1}$. Winter deviation from the daily mean of the diurnal trend of the rainfall has a broad maximum from 0000 to 0900, with a broad minimum from 1200 to 1800. Spring does not have a distinct variation except for the largest maximum at 0300 and the lowest minimum at 1200. Summer rainfall, however, does have a diurnal variation with a maximum centered between 0300 and 0600. Finally, the fall is rather confused with maxima at 0000 and 0600 in addition to the minimum at 1200.

7. Summary

Meteorological and oceanographic variables were analyzed based upon 20 years and 7 years of data, respectively. These variables, which include sea temperature, air temperature, dew point, rain, wind speed, pressure, mixed layer depth, and surface density all have a significant seasonal trend. Another variable, the total cloud cover, has only a weak seasonal trend with a yearly average of about 5/8. Most of the cloud cover is due to low stratiform clouds. As the surface salinity does not have a significant seasonal trend, and the surface density does, it is concluded that the salinity does not have a significant effect on the seasonal surface density. In addition to the seasonal trend, the surface pressure has a local maximum at the end of December and early January. The yearly average rainfall is 23 cm, less than half previous estimates.

The cross section of temperature with depth is as expected with the large seasonal changes in the near surface. The salinity cross section does not have a significant seasonal trend. A cross section of density appears similar to the temperature, and it is concluded that the seasonal trend of the subsurface density is a function of temperature.

Variation of the surface heat balance also shows a seasonal trend. However, the two decades studied have distinctly different balances, with the 1961–70 decade having a smaller negative balance than the 1951–60 decade. This heat balance change coincides with a large-scale climatic change in the North Pacific (Namias, 1969).

For the 20-year record some large pressure anomalies seem to be correlated with abnormally heavy rainfall in the equatorial Pacific. The rainfall and the difference between sea and air temperature appear to reflect the large-scale climatic changes of 1957–58 when a large El Niño occurred.

Sea temperature, air temperature, dew point, pressure, wind speed, and total cloud cover all have distinct diurnal trends. Wind speed, rainfall, and total cloud cover also have significantly different diurnal trends during each of the four seasons.

Acknowledgment. Oceanographic data came from the National Oceanographic Data Center, and meteorological data from the National Climatic Center. This work was supported by the Atmospheric Sciences

Section of the National Science Foundation under Grants GA-1571 and GA-27205.

REFERENCES

Bathen, K. H., 1972: On the seasonal change in the depth of the mixed layer in the North Pacific Ocean. *J. Geophys. Res.*, **77**, 7138–7150.

Berlyand, T. G., 1960: Method of climatological calculation of global radiation. *Meteor. Gidrol.*, **6**, 9–12.

Bjerknes, J., 1969: Atmospheric teleconnections from the equatorial Pacific. *Mon. Wea. Rev.*, **97**, 163–172.

Budyko, M. I., 1956: *The Heat Balance of the Earth's Surface.* Leningrad, Gidrometeor. (Translated by Office of Technical Service, U. S. Dept. of Commerce, Washington, D. C., 1958, 259 pp).

Deardorff, James, 1968: Dependence of air-sea transfer coefficients on bulk stability. *J. Geophys. Res.*, **73**, 2549–2557.

Husby, David M., 1969: Oceanographic observations, North Pacific Ocean Station *November*, 30°00N 140°00W, March 1967–March 1968. Oceanogr. Report. No. 26 CG-373-26, U. S. Coast Guard.

Jacobs, W. C., 1951: The energy exchange between the sea and the atmosphere and some of its consequences. *Bull. Scripps. Inst. Oceanogr.*, **6**, 27–122.

Malkus, J. S., 1962: Large-scale interactions. *The Sea*, Vol. 1, New York, Interscience, 88–294.

Namias, Jerome, 1959: Recent seasonal interactions between North Pacific waters and the overlying atmospheric circulation. *J. Geophys. Res.*, **64**, 631–646.

——, 1969: Seasonal interactions between the North Pacific Ocean and the atmosphere during the 1960's. *Mon. Wea. Rev.*, **97**, 173–192.

Quinn, William H., and Wayne V. Burt, 1972: Use of the southern oscillation in weather prediction. *J. Appl. Meteor.*, **11**, 616–628.

Reed, R. K., and William P. Elliott, 1973: Precipitation at ocean weather stations in the North Pacific. *J. Geophys. Res.*, **78**, 7087–7091.

Roll, H. V., 1965: *Physics of the Marine Atmosphere.* New York, Academic Press, 426 pp.

Sverdrup, H. V., M. W. Johnson and R. H. Flemming, 1942: *The Oceans, Their Chemistry, Physics, and General Biology.* New York, Prentice-Hall, 1087 pp.

Tucker, G. B., 1961: Precipitation over the North Atlantic Ocean. *Quart. J. Roy. Meteor. Soc.*, **87**, 147–158.

Tully, J. P., 1964: Oceanographic regions and processed in the seasonal zone of the North Pacific Ocean. *Studies on Oceanography*, Kozo Yoshida, Ed., University of Washington Press, 58–84.

—— and L. F. Giovando, 1963: Seasonal temperature structure in the eastern subarctic Pacific Ocean. M. J. Dunbar, Ed., The Royal Society of Canada Spec. Publ. No. 5, 10–36.

U. S. Naval Hydrographic Office, 1961: *Climatological and Oceanographic Atlas for Mariners. Vol. II., North Pacific Ocean.* Washington, D. C., Govt. Printing Office. 159 pp.

Wyrtki, Klaus, 1965: The average annual heat balance of the North Pacific Ocean and its relation to ocean circulation. *J. Geophys. Res.*, **70**, 4547–4559.